Proceedings of the 28th IEEE
EMBS Annual International Conference
New York City, USA, Aug 30-Sept 3, 2006

Characterization of carotid atherosclerotic plaques using frequency-based texture analysis and bootstrap

J. Stoitsis, N. Tsiaparas, S. Golemati, and K. S. Nikita
Department of Electrical and Computer Engineering, National Technical University of Athens, Greece

Abstract— **Texture analysis of B-mode ultrasound images of carotid atheromatous plaque can be valuable for the accurate diagnosis of atherosclerosis. In this paper, two frequency-based texture analysis methods based on the Fourier Power Spectrum and the Wavelet Transform, were used to characterize atheromatous plaques. B-mode ultrasound images of 10 symptomatic and 9 asymptomatic plaques were interrogated. A total of 109 texture features were estimated for each plaque. The bootstrap method was used to compare the mean values of the texture features extracted from the two groups. After bootstrapping, three features were found to be significantly different between the two types of plaques: the average value of the angular distribution corresponding to the wedge centered at 90^0, the standard deviation at scale 1 derived from the horizontal detail image, and the standard deviation at scale 2 derived from the horizontal detail image. It is concluded that frequency-based texture analysis in combination with a powerful statistical technique, such as bootstrapping, may provide valuable information about the plaque tissue type.**

Keywords—**Carotid atherosclerosis, ultrasound imaging, texture analysis, Fourier Power Spectrum, Wavelet Transform**

I. Introduction

It has been shown that the instability of the carotid atheromatous plaque may be associated not only with the degree of stenosis but also with plaque echogenicity estimated from B-mode ultrasound images [1]. Plaque echogenicity via image texture analysis has been analyzed with a number of techniques. Texture features derived from statistical [2], [3], model-based [4], [3] and Fourier-based [3] methods have been used to characterize and classify carotid atheromatous plaques from B-mode ultrasound.

Frequency-based texture analysis, including Fourier and Wavelet Transforms, has been used to characterize biological tissue from medical images. Fourier-based texture features have been estimated for carotid artery plaques from ultrasound images [2] and for coronary artery plaques from intravascular ultrasound [5]. The two-dimensional Wavelet Transform (WT) is an efficient mathematical tool for texture analysis of medical images. It has been shown that the scale/frequency approach based on the WT is appropriate for texture feature extraction from ultrasound images [6]. Wavelet-based texture analysis using the Haar wavelet has been used to differentiate viable from non-viable myocardium from echographic images [7].

Previous work on texture analysis of atheromatous plaque includes the use of classification and traditional statistical analysis under the assumption that the original sample is sufficiently large to apply 'asymptotic' results. The bootstrap technique was introduced as an approach to estimate confidence intervals for parameters in cases for which standard statistical methods cannot be applied [8]. The technique can be used for the estimation of statistical measures without any assumptions about the distribution of the original data. The bootstrap method is extremely valuable in situations where the original data size is small. Recently, the bootstrap technique was used to assist the differential diagnosis of solid breast tumors using small training sets [9].

The purpose of this paper was to investigate the efficiency of frequency-based texture analysis techniques to characterize carotid atherosclerotic plaques from B-mode ultrasound. Furthermore, the use of the bootstrap technique allows validating the texture analysis results.

II. Methodology

A. Subjects and Procedures for Acquisition and Pre-processing of Images

A total of 19 atheromatous plaques were investigated, of which 10 were symptomatic and 9 asymptomatic. Symptoms included stroke, hemispheric transient ischemic attack and amaurosis fugax. There was no significant difference in the degrees of stenosis between the two groups of plaques (Student's t-test, p-value=0.93).

For each subject, a sequence of longitudinal images was recorded with an ATL (Advanced Technology Laboratory) Ultramark 4 Duplex scanner and a high resolution 7.5 MHz linear scan head. Scanner settings (dynamic range 60dB, 2D grey map, persistence low, frame rate high) were set at the beginning of the recording and not altered during the

1-4244-0033-3/06/$20.00 ©2006 IEEE.

procedure. These settings were common for all investigations. Figure 1 shows examples of images from a symptomatic and an asymptomatic subject in which the regions of interest (ROIs), corresponding to plaques, were outlined by an expert. It is pointed out that, although the Figure shows histogram-equalized images, Fourier- and Wavelet-based texture analysis was performed on the original (non–histogram-equalized) image ROIs.

B. Texture Analysis from B-mode Ultrasound Images

Texture analysis from B-mode ultrasound images was performed using ANALYSIS, a modular software system designed to assist interpretation of medical images [10]. The main steps of the two frequency-based texture analysis approaches, namely Fourier Power Spectrum (FPS) and WT, are described below.

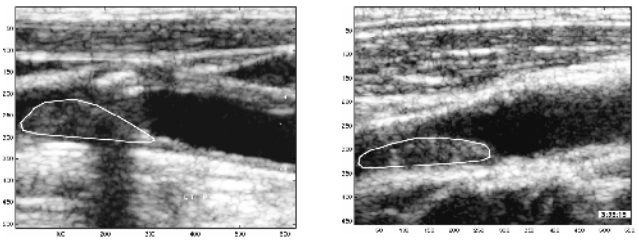

Fig. 1. Examples of B-mode ultrasound images of (a) an asymptomatic and (b) a symptomatic carotid atheromatous plaque. The numbers correspond to the number of pixels from the top and left sides of the image. The plaque boundary was outlined by an expert on the histogram equalized version of the image, because this version enhances visualization of structures of interest.

Fourier Power Spectrum: Quantifying image texture in the frequency domain is based on the discrete 2-D Fourier Transform (FT). If F is the FT of an image, its FPS is $|F|^2$. It is well known that the radial distribution of the values in FPS is sensitive to texture coarseness in an image and that their angular distribution is sensitive to the directionality of the texture. Power concentration in low spatial frequencies indicates coarse texture while power concentration in high frequencies indicates fine texture. Moreover, texture with strong directional characteristics produces a power spectrum concentrated along lines perpendicular to the texture direction.

Two sets of texture features were extracted from the FPS [11]. The first set corresponds to the radial distribution of the power spectrum and the second set to the angular distribution. For the radial distribution, ring-shaped samples of the power spectrum were used:

$$\textit{Radial Distribution: } \frac{1}{N^2} \sum_{\substack{r_1^2 < i^2 + j^2 < r_2^1 \\ 1 \le i, j \le N}} \left| F(i, j) \right|^2$$

where F(i, j) is the FT of the NxN image, and r_1, r_2 are the inner and outer radii of the ring, respectively.

The angular distribution of the power spectrum is based on the estimation of wedge-shaped samples:

$$\textit{Angular Distribution: } \frac{1}{N^2} \sum_{\substack{\theta_1 \le tan^{-1}(j/i) \le \theta_2 \\ 1 \le i, j \le N}} \left| F(i, j) \right|^2$$

where θ_1, θ_2 are the lower and upper limit of the wedge.

For each plaque, 9 texture features based on the FPS were estimated. In particular, for radial distribution five ring samples were used resulting in five texture features. The mean value of the ring size was 12.5 pixels. For the angular distribution, the wedges used were 45^0 wide, centered at 0^0, 45^0, 90^0 and 135^0. Thus, four texture features characterizing the angular distribution of the power spectrum were extracted. In Fig. 2, the ROI corresponding to an atheromatous plaque and its FPS are shown.

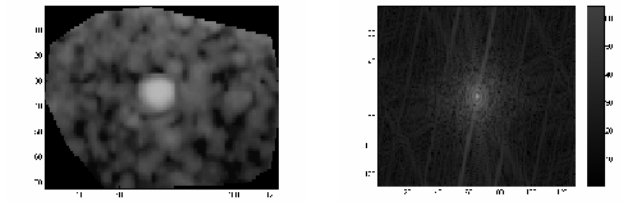

Fig. 2. (a) ROI corresponding to atheromatous plaque and (b) power spectrum of the selected ROI. The zero frequency was shifted to the center of the spectrum

Wavelet Transform: The data provided by the intensities of an array of pixels that make up an image are in two dimensional form. In order to perform a wavelet-based parametric characterization for texture image analysis two dimensional discrete wavelet transforms must be used. In this way we can extract information about the low and high frequencies of an image at every resolution. Therefore, if the frequency spectrum is decomposed appropriately, different textures will result into different features. The 2D wavelet transform is actually two separate 1D wavelet transforms. The first transform is performed along each row of the image. The second transform is performed on each column of the resulting image. The wavelet coefficients obtained are called the sub-images at every resolution. These sub-images are basically an approximation image and three detail images, namely the horizontal, vertical and diagonal detail images (Fig. 3). By adding the image details at an arbitrary scale to the approximation image at that scale we obtain the image approximation at an increased resolution (i.e. at a smaller scale). This is the so called multiresolution representation [12].

The following features characterizing image texture were extracted from the wavelet coefficients:

$$\textit{Wavelet Signature Energy: } \frac{1}{N^2} \sum_{i,j=1}^{N} C_s^d(i, j)^2$$

$$\textit{Shannon Entropy: } -\frac{1}{N^2} \sum_{i,j=1}^{N} C_s^d(i, j) \log C_s^d(i, j)$$

Standard deviation: $\sqrt{\frac{1}{N^2}\sum_{i,j=1}^{N}\left(C_s^d(i,j)-Mean\right)^2}$

and the co occurrence features [13]:

Cluster Prominence: $\frac{1}{N^2}\sum_{i,j=1}^{N}(i-M_x+j-M_y)^4 C_s^d(i,j)$

Cluster Shade: $\frac{1}{N^2}\sum_{i,j=1}^{N}(i-M_x+j-M_y)^3 C_s^d(i,j)$

where

$Mean=\frac{1}{N^2}\sum_{i,j=1}^{N}C_s^d(i,j)$,

$Mx=\sum_{i,j=1}^{N}iC(i,j)$, $My=\sum_{i,j=1}^{N}jC(i,j)$

and $C_s^d(i,j)$ are the wavelet coefficients for $d = h, v, d, t$ (horizontal, vertical, diagonal and total) at scale $s = 1,2,\ldots,5$.

Each NxN image was decomposed up to 5 scales using an orthogonal, near symmetric and compactly supported mother wavelet, the symlet20 [14]. The choice of the mother wavelet is critical and, because these images present rapid intensity fluctuations, a tight wavelet must be used. The approximation sub-images were not used for texture analysis because they are just a rough estimate of the original image and capture the variations induced by lighting and illumination. Hence, a total of 100 wavelet-based texture features were extracted for each plaque.

C. Statistical Analysis of Texture Features

To determine the discriminatory value of each texture feature, a simple statistic figure of merit corresponding to the distance between the two groups was used:

$$dis=\frac{|m_1-m_2|}{\sqrt{\sigma_1^2+\sigma_2^2}}$$

where m_1, m_2 are the mean values and σ_1, σ_2 the standard deviations of the two groups. Features that produced *dis* value greater than a set threshold (in this study 0.57 was used as threshold) were retained while the remaining were discarded.

Bootstrap: The bootstrap method was used to compare the mean values of the texture features extracted from the two investigated groups, i.e., symptomatic and asymptomatic. 10000 bootstrap samples were generated from the original data and the difference of the mean value of samples was used as the statistic to compare the two investigated groups. The statistic was estimated for all the samples and the distribution of the statistic was determined. The proportion of the samples that had a statistic value greater than the actual observed value of the statistic was used to determine the p-value of the bootstrap statistical test.

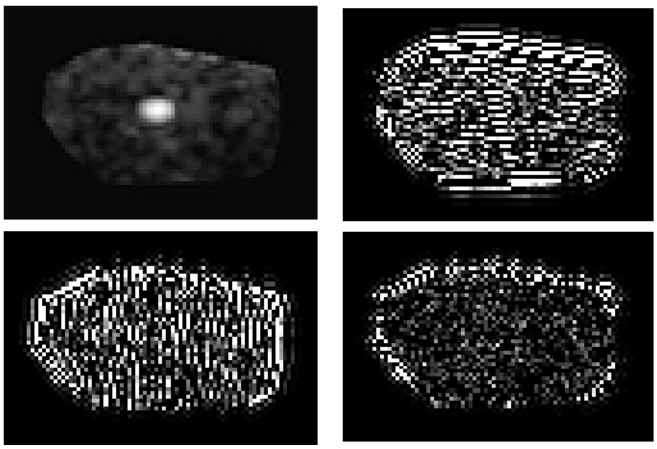

Figure 3: Example of wavelet decomposition of a B-mode ultrasound image of an atheromatous plaque: Approximation image (upper left), Horizontal detail image (upper right), Vertical detail image (low left) and Diagonal detail image (low right). All images correspond to scale 1.

III. RESULTS

A total of 109 texture features (9 Fourier- and 100 Wavelet-based features) were estimated for each plaque. Three FPS-based and five WT-based texture features had the highest distance values. The FPS-based texture features included the average value of the radial distribution for the fourth ring (RD4), the average value of the radial distribution for the fifth ring (RD5) and the average value of the angular distribution corresponding to the third wedge (AD3). The WT-based texture features with high distance values included the standard deviation at scale 1 derived from the horizontal detail image (STD1h), the standard deviation at scale 1 derived from the horizontal detail image (STD2h), the cluster shade at scale 1 derived from the diagonal detail image (CLSH1d), the sum value of standard deviation at scale 2 (STD2s) and the entropy at scale 5 derived from the vertical detail image (ENTR5v). Table 1 shows the average values (± standard deviations) of these features as well as the corresponding distance values.

After comparing the two groups using the bootstrap method, only three features were found to be significantly different (significance level p=0.05). These included the AD3 that is centered at 90^0, the STD1h and the STD2h. In Table 1, the p-values estimated using the bootstrap statistic test are shown.

As we can see, the texture feature that describes the angular distribution at the direction of 90^0 was found significantly lower in asymptomatic subjects. This feature had the highest distance value and the lowest p-value. It should be

pointed out that a texture with high directional information at an angle θ produces peaks of angular distribution in θ+π/2. The estimated distance values of the radial distribution for the fourth and fifth ring were relatively high, but they did not reach statistical significance. These features were lower in asymptomatic plaques.

Among the WT-based features, STD1h and STD2h were significantly lower in asymptomatic subjects. ClSh1d, STD2s and ENTR5v were also lower in asymptomatic subjects, but they did not reach statistical significance.

TABLE 1. STATISTICAL ANALYSIS OF TEXTURE FEATURES OF SYMPTOMATIC AND ASYMPTOMATIC PLAQUES. DIS DISTANCE.

Texture Feature	Symptomatic	Asymptomatic	dis	Bootstrap p-value
Fourier Power Spectrum				
RD4	41.55±8.33	35.25±5.60	0.628	0.063
RD5	36.97±8.18	31.11±5.26	0.579	0.08
AD3	46.21±9.01	37.21±6.73	0.799	0.027
Wavelet Transform				
STD1h	1.63±0.51	1.12±0.53	0.698	0.042
STD2h	3.81±0.96	2.74±1.07	0.745	0.032
ClSh1d	236.27±648.06	-886.04±1947.6	0.586	0.079
STD2s	4.21±1.07	3.20±1.39	0.576	0.086
ENTR5v	-1.59e+08 ±1.35e+08	-8.30e+08 ±1.22e+09	0.616	0.059

IV. DISCUSSION

In the small group of images that were investigated in this study, three texture features were found to significantly differentiate between symptomatic and asymptomatic plaques. The feature with the lowest p-value (AD3) was a FPS-based feature; this suggests that texture periodicity, estimated using the 2D FT may be useful for the characterization of atheromatous plaque. Furthermore, the two significantly different WT-based features were calculated from the horizontal sub-image at scales 1 and 2. This image is derived after computing the trends of the initial image along rows (low-pass filtering) followed by the computation of the fluctuations along its columns (high-pass filtering).

All three features corresponded to texture patterns in the horizontal direction, indicating that horizontal texture patterns may better characterize atheromatous plaque tissue. This may be related to the direction of stresses exerted on the plaques and the corresponding strains; mainly, these occur in directions along the axis of the artery.

In addition to this, features that describe high spatial frequency texture patterns were also found to characterize somewhat efficiently the plaque tissue.

V. CONCLUSION

This study has demonstrated that frequency-based texture analysis can be used to characterize carotid atherosclerotic plaques from B-mode ultrasound. The application of bootstrapping in the small group of images that were investigated allows the extraction of valid conclusion about the discriminatory value of the texture features.

ACKNOWLEDGMENT

Special thanks are due to Professor Andrew N.Nicolaides and the staff of the Irvine Laboratory, St. Mary's Hospital, London, for their contribution in recording the image sequences.

REFERENCES

[1] M. L. Grønholdt., B. G. Nordestgaard, T. V. Schroeder, S. Vorstrup, and H. Sillesen, "Ultrasonic echolucent carotid plaques predict future strokes," *Circulation*, vol. 104, no. 1, pp. 68-73, 2001.

[2] J. E. Wilhjelm, M. L. M. Grønholdt, B. Wiebe, S. K. Jespersen, L. K. Hansen, H. Sillesen, "Quantitative analysis of ultrasound B-mode images of carotid atherosclerotic plaque: correlation with visual classification and histological examination," *IEEE Trans. Med. Imag.,* vol. 17, no. 6, pp. 910-922, Dec. 1998.

[3] C. I. Christodoulou, C. S. Pattichis, M. Pantziaris, and A. N. Nicolaides, "Texture-based classification of atherosclerotic carotid plaques," *IEEE Trans. Med. Imaging*, vol. 22, no. 7, pp. 902-912, Jul. 2003.

[4] P. Asvestas, S. Golemati, G. K. Matsopoulos, K. S. Nikita, A. N. Nicolaides, "Fractal dimension estimation of carotid atherosclerotic plaques from B-mode ultrasound: a pilot study," *Ultrasound Med. Biol.*, vol. 28, no. 9, pp. 1129-1136, Sep. 2002.

[5] D. G. Vince, K. J. Dixon, R. M Cothren, J. F. Cornhill, "Comparison of texture analysis methods for the characterization of coronary plaques in intravascular ultrasound images," *Comput. Med. Imaging Graph.*, vol. 24, no. 4, pp. 221-229, 2000.

[6] A. Mojsilovic, M. V. Popovic, A. N. Neskovic, and A. D. Popovic, "Wavelet image extension for analysis and classification of infarcted myocardial tissue," *IEEE Trans. Biomed. Eng*., vol. 44, no. 9, pp. 856-866, 1997.

[7] A. N. Neskovic, A. Mojsilovic, T. Jovanovic, J. Vasiljevic, M. Popovic, J. Marinkovic, M. Bojic, and A.D. Popovic "Myocardial tissue characterization after acute myocardial infarction with wavelet image decomposition: a novel approach for the detection of myocardial viability in the early post infarction period," *Circulation*, vol. 98, no. 7, pp. 634-641, 1998.

[8] B. Efron, R. J. Tibshirani, An Introduction to the Bootstrap New York, Chapman & Hall, 1993.

[9] D. R. Chen, W. J. Kuo, R. F. Chang, W. K. Moon and C. C. Lee, "Use of the bootstrap technique with small training sets for computer-aided diagnosis in breast ultrasound," *Ultrasound Med. Biol*., vol. 28, no. 7, pp. 897–902, 2002

[10] J. Stoitsis, S. Golemati, K. S. Nikita, "A modular software system to assist interpretation of medical images – Application to vascular ultrasound images", *Trans. Instrum. Meas.*, Dec. 2006. (in press)

[11] J. S. Weszka, C. R. Dyer, and A. Rosenfield, "A comparative study of texture measures for terrain classification," *IEEE Trans. Syst., Man, Cybern*., vol. SMC-6, pp. 269-285, Apr. 1976.

[12] I. Daubechies, "Ten lectures on wavelets," CBMS, SIAM, vol. 61, pp. 258-261, 1994.

[13] S. Arivazhagan, L. Ganesan, "Texture classification using wavelet transform," Pattern Recogn. Lett., vol. 24, pp. 1513 – 1521, 2003.

[14] M. H. Bharati, J. J. Liu, J. F Macgregor, "Image texture analysis: methods and comparisons," Chemometr. Intell. Lab., vol. 72, no. 1, pp. 57– 71, 2004.